Supplementary Information for

Domain knowledge-guided interpretive machine learning: Formula discovery for the oxidation behavior of ferritic-martensitic steels in supercritical water

Author Information

Affiliations

Materials Genome Institute, Shanghai University, Shanghai 200444, China

Bin Cao-1, Shuang Yang-2, Ankang Sun-3, Ziqiang Dong-4, Tong-Yi Zhang-5

Corresponding authors

Correspondence to: Tong-Yi Zhang-5, Ziqiang Dong-4

zhangty@shu.edu.cn (Tong-Yi Zhang); zqdong@shu.edu.cn (Ziqiang Dong)

This supplementary material includes:

An introduction of TCLR

Figures S1-S4

Tables S1-S5

Reference (1-22)

A github site for sharing the code

Contents

1 TCLR model

1.1 Background

Tree-Classifier for Linear Regression (TCLR) [1] is a novel tree algorithm developed for capturing the functional relationships between features and target, through partitioning the feature space into a set of sub-domains, and embodying a specific function on each of subdomains. It is conceptually simple yet powerful for distinguishing mechanisms. The entire feature space is divided into the sub-domains by hyperplanes parallel to the feature coordinate axes. In each leaf of a grown TCLR tree, target y is a prior function of features $x_{\hat{j}}$ $(\hat{j} = 1, \cdots, \hat{m})$ $\hat{m} \leq m$, which is a subset of features $(x_1, \cdots, x_m)$. Linear function is considered in the present work and features $x_{\hat{j}}$ are called linear features. TCLR has the function to screen data which do not follow the prior function. In each splitting, TCLR chooses a feature and a split-point from data $\{x_{ij}\}(\mathrm{i} = 1, \cdots, \mathrm{n})(\mathrm{j} = 1, \cdots, \mathrm{m})$ to let data in one or both sub-domains be more biased the prior function than their parent node, and recursively binary partitions the split-feature space, until some stopping rules are applied.

1.2 How to grow a TCLR tree

TCLR can automatically decide on split feature and split-point from data $\{x_{ij}\}(\mathrm{i} = 1, \cdots, \mathrm{n})(\mathrm{j} = 1, \cdots, \mathrm{m})$ with a mature criterion for splitting and pruning the tree. In each leaf, the response is a prior function of features $x_{\hat{j}}$ $(\hat{j} = 1, \cdots, \hat{m})$ $\hat{m} \leq m$, $y = f(x_{\hat{j}})$, where f is the "prior function" proposed by domain knowledge.

In the present work, the maximal Linearity Goodness is used to find the best partition in each splitting. The following LG metrics are used in TCLR.

The Pearson Correlation Coefficient (ρ),

$$\rho = \frac{\sum_{i=1}^{n}(x_{i\hat{j}}-\overline{x_{\hat{j}}})(y_i-\bar{y})}{\sqrt{\sum_{i=1}^{n}(x_{i\hat{j}}-\overline{x_{\hat{j}}})^2 \sum_{i=1}^{n}(y_i-\bar{y})^2}}, \tag{S1.1}$$

measures the linearity goodness between the target and linear-feature $x_{\hat{j}}$, where $x_{i\hat{j}}$ denotes the value of feature $\hat{j}$ on datum i. The coefficient of determination of R-Square (R^2),

$$R^2 = 1 - \frac{\sum_{i=1}^{n}(x_{i\hat{j}}-\bar{y})^2}{\sum_{i=1}^{n}(x_{i\hat{j}}-\overline{x_{\hat{j}}})^2}, \tag{S1.2}$$

gauges the prediction goodness of a ML model. The Maximal Information Coefficient (MIC) [2],

$$I(x_{\hat{j}}, y) = \sum_{i=1}^{l}\sum_{j=1}^{k} P(x_{\hat{j}} = a_i, y = b_j) log \frac{P(x_{\hat{j}}=a_i, y=b_j)}{P(x_{\hat{j}}=a_i)P(y=b_j)}, \tag{S1.3}$$

measures the general correlation, linear and nonlinear, between the target and feature where $a \in \{a_1, a_2, \cdots, a_l\}(l \le n)$ denotes l bins of variable $x_{\hat{j}}$ and $b \in \{b_1, b_2, \cdots, b_k\}(k \le n)$ denotes k bins of response y.

In addition to the metrics introduced above, the Mean Absolute Percentage Error (MAPE) is also used to evaluate ML models, which is defined by

$$MAPE = \frac{1}{n}\sum_{i=1}^{n}\frac{|\hat{y}_i - y_i|}{y_i}. \tag{S2}$$

where n is the number of data, y_i is the true value and $\hat{y}_i$ is the prediction.

Starting with all the n data $\{x_{ij}\}(\mathrm{i} = 1, \cdots, \mathrm{n})(\mathrm{j} = 1, \cdots, \mathrm{m})$ and considering a split-variable j and split-point value i, and a child node pair of $R^l(x_j \le i)$ and $R^r(x_j > i)$, we determine the optimal split-pair by

$$\max_{i,j}[\frac{1}{2}\left(\underset{R^l}{\mathrm{LG}}(x_{\hat{j}}, f) + \underset{R^r}{\mathrm{LG}}(x_{\hat{j}}, f)\right) - \underset{R^l+R^r}{\mathrm{LG}}(x_{\hat{j}}, f)] \tag{S3}$$

TCLR treats the positive and negative linearity separately to avoid any potential mixture of both in a splitting. The pseudo-program for a linear prior is given below.

Algorithm: TCLR

---

fit Dataset $S = \{x_{ij}\}(i = 1, \cdots, \mathrm{n})(j = 1, \cdots, \mathrm{m})$

produce CHOOSE split point set $\{x_{ij}\}$ (i for 1~n, j for 1~m)

best feature $=-1$

best value $=-1$

ΔLG=0

For x_{IJ} in $\{x_{ij}\}$

produce Sub-dataset $\{S_l(x_j \leq i), S_l(x_j > i)\}$,

If $\frac{|\rho(x_{\hat{j}}^l, f^l) + \rho(x_{\hat{j}}^r, f^r)|}{2} - |\rho(x_{\hat{j}}, f)| \geq \max(\Delta LG, |\mathrm{mininc}|)$

return $\Delta LG = \frac{|\rho(x_{\hat{j}}^l, f^l) + \rho(x_{\hat{j}}^r, f^r)|}{2} - |\rho(x_{\hat{j}}, f)|$

best split-feature = j

best split-value = i

end if

end for

return (i, j)

end produce

TCLR tree must be pruned, obviously a very large tree might overfit the data, while a small one might not capture important information. Thus, tree size is a tuning parameter governing the model's complexity. Let $|T|$ denote the number of terminal nodes and LG_m denote the LG on the m-th leaf. We define the utility criteria as:

$$U(TCLR) = \sum_{m=1}^{|T|} LG_m - \beta|T| \quad \text{(S4)}$$

The tuning parameter $\beta \geq 0$ governs the trade-off between tree size and its fitting goodness. For each β, there is a unique tree. β is regulated by three parameters in TCLR, viz.,

>>> [|mininc|] (default=0.01),

viz., the allowed minimum increment of Gain Function of Eq.(S3). If $\Delta LG \leq |\mathrm{mininc}|$, the node will become a leaf.

>>> [|Threshold|] (default=0.95),

when LG in a node is equivalent to or higher than the present threshold, the node will become a leaf.

>>> [minsize] (default=3),

the amount of data in a leaf shouldn't be smaller than the minimum size.

TCLR is implemented on the desktop platform and a Graphical User Interface (GUI) is developed for it. The relevant software and source code are fully open which is available in section 3.

2 Supplementary Tables and Figures

2.1 Optimized values of hyperparameters

The 10-fold cross-validation and the Xgboost algorithm with random_state=99 in the Application Programming Interface (API) and python library scikit-learn [3] were employed to establish models with the optimal hyperparameters listed in Table S1.

Table S1. Optimal hyperparameters used in each model

model	n_estimators	learning_rate	random_state in CV	ρ
on 15 raw features (184)	399	0.18	99	0.921
on 15 converted features (184)	99	0.44	87	0.948
on 15 converted features (178)	80	0.31	16	0.986
on 8 converted features (178)	95	0.22	95	0.988
on 4 features (178)	92	0.38	289	0.985

2.2 The SHAP values of alloying elements

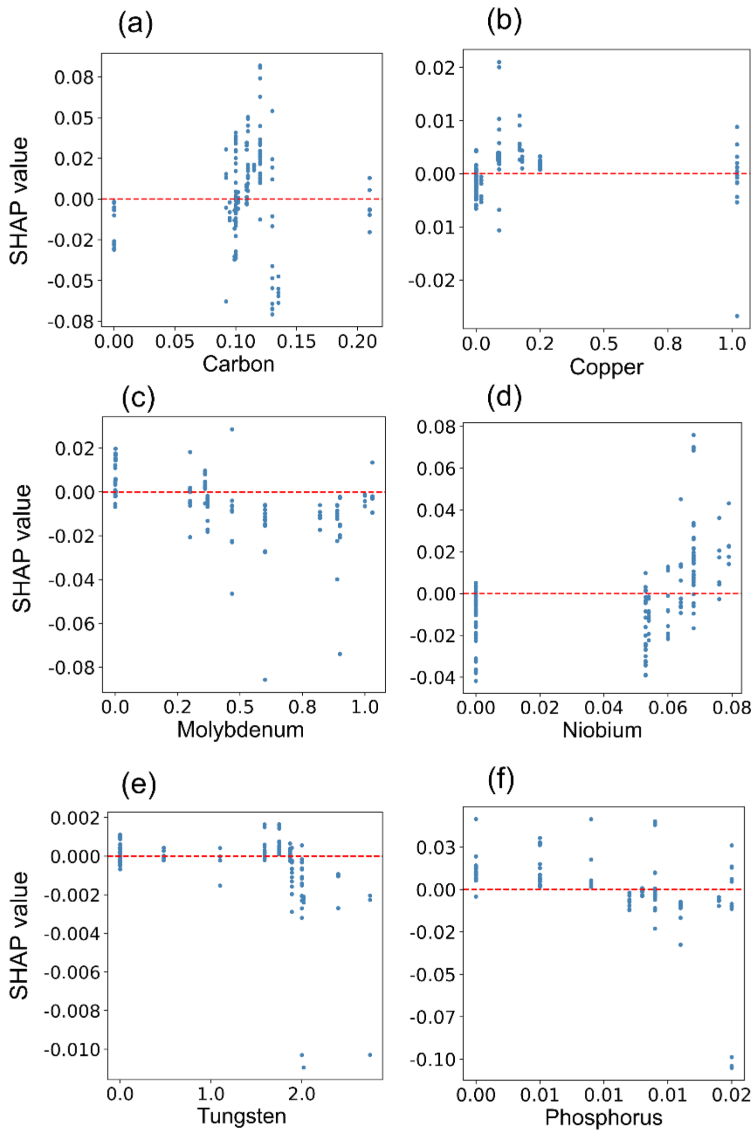

Figure S1. (a~f) The SHAP values of alloying elements of C, Cu, Mo, Nb, W, and P.

2.3 Comparison of PF1 and PF2

Let $\Delta w = f(T, t, \mathrm{DOC}, \mathrm{G})$ denote as payoff function one (PF1) and $\ln\left(\frac{\Delta w}{\Delta w_{00}}\right) = f\left(\frac{1}{RT}, ln\left(\frac{t}{t_0}\right), \mathrm{DOC}, \mathrm{G}\right)$ denote as payoff function two (PF2), where G represents the influence of alloying elements.

Figure S2(a, b) and Figure S2 (c, d) shows the Xgboost predictions (with all 184 data) and the error histograms for PF1 and PF2, respectively, clearly indicating that the prediction accuracy increases from ρ=0.921 for PF1 to ρ=0.948 for PF2 and the error probability distribution for PF2 is closer to the normal distribution with mean of zero.

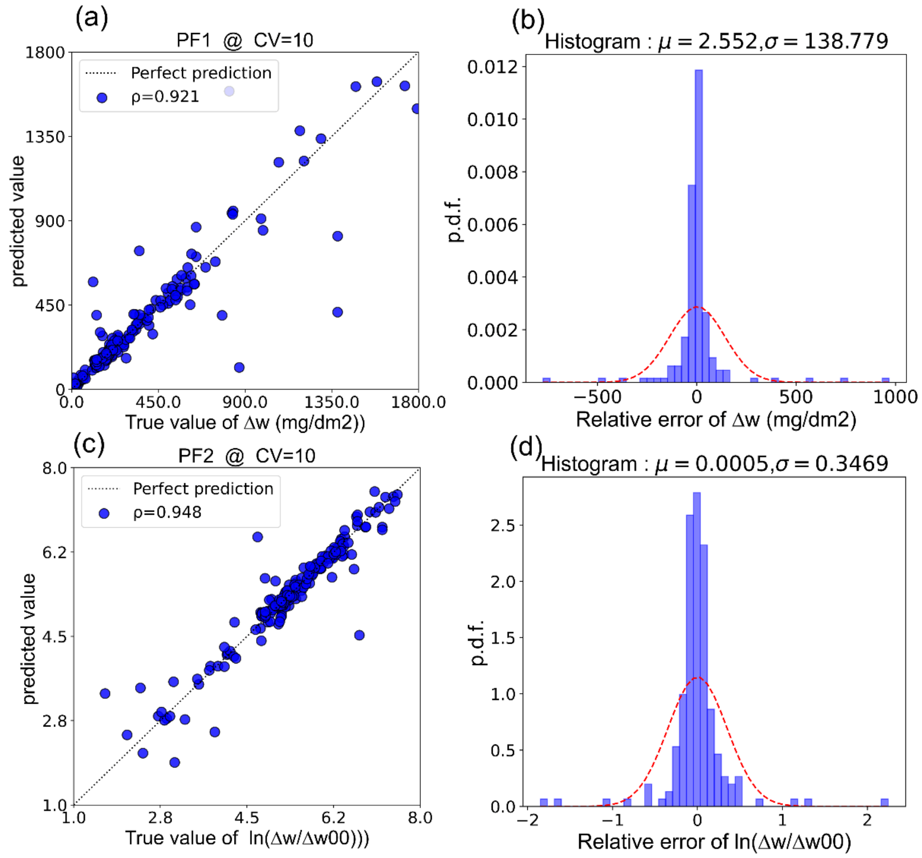

Figure S2. (a, c) Experimental values versus predicted values, (b, d) the error probability density functions, (a, b) for PF1 and (c, d) for PF2.

2.4 Outliers

The 3σ criterion is taken as the threshold to gauge whether a datum is an outlier, which gives the outliers of number 5 (ref.[4]), 67 (ref.[5]), 88 (ref. [4]), 89 (ref. [4]), 99 (ref. [4]) and 184 (ref.[5]), highlighted in the FMO dataset.

Data 88, 89 and 99 share the same testing temperature of 360°C (Pressure=25MPa) below the critical temperature of SCW. Data 5, 67, and 184 are exposed to very high pressure on 30, 31 and 31MPa, respectively. When the pressure reaches 30MPa or greater, the oxide layer will become thicker, affecting the diffusion of Cr element. The three data are treated as outliers and moved out in the present study.

2.5 Multiple values of ln(w/w00)

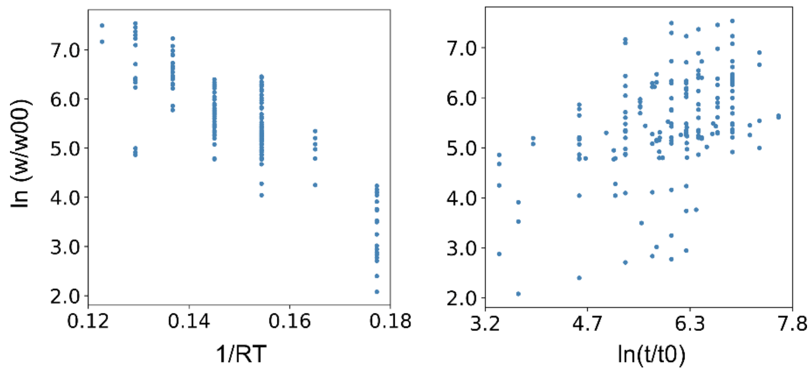

Figure S3. The plots of $ln\frac{\Delta w}{\Delta w_{00}}$ versus $\frac{1}{RT}$ and $ln\frac{\Delta w}{\Delta w_{00}}$ versus $\ln\left(\frac{t}{t_0}\right)$. Multiple values of $ln\frac{\Delta w}{\Delta w_{00}}$ for a given value of $\frac{1}{RT}$ or $\ln\left(\frac{t}{t_0}\right)$ due to the contributions of other features.

2.6 The results of TCLR

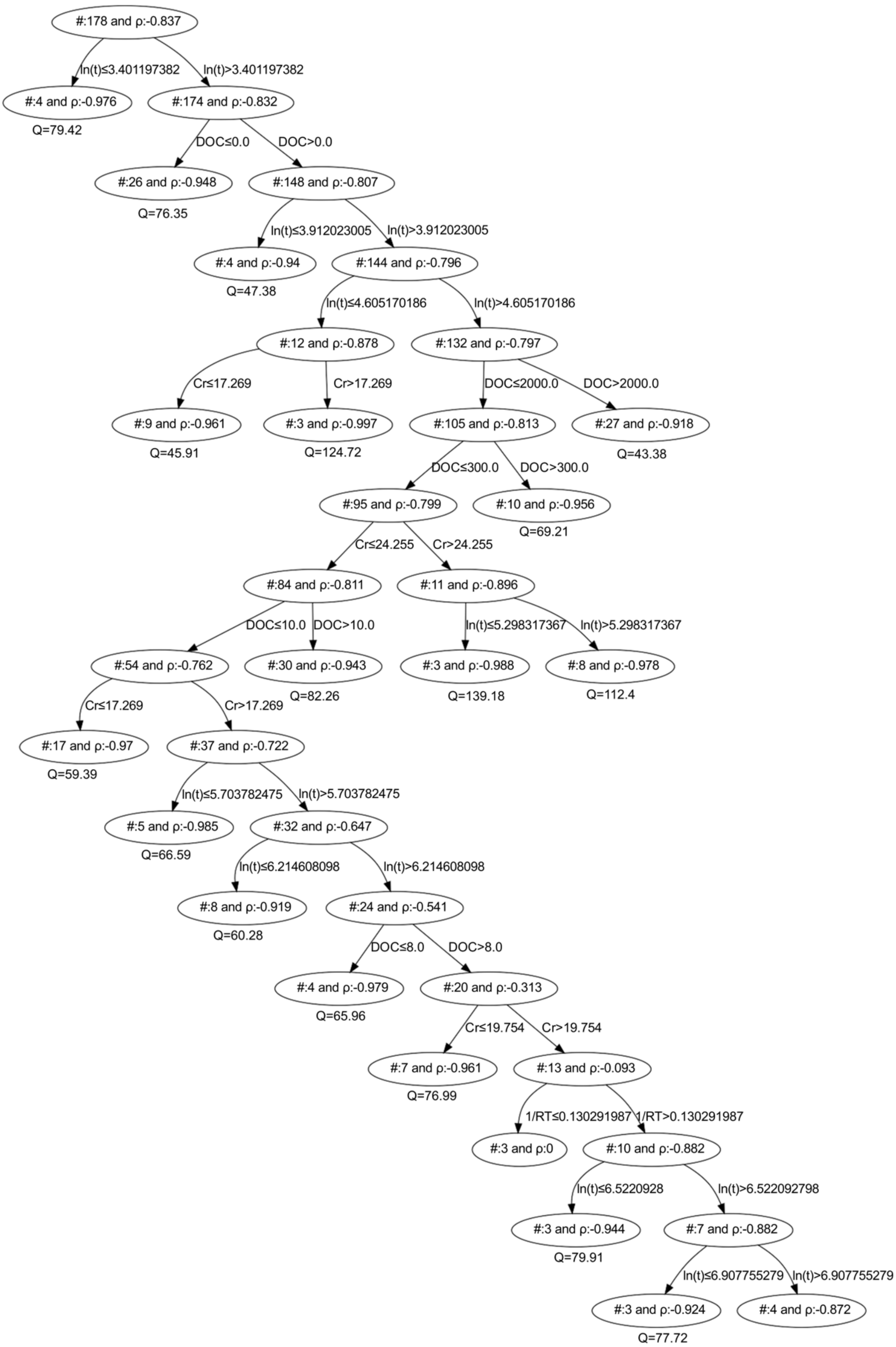

(a)

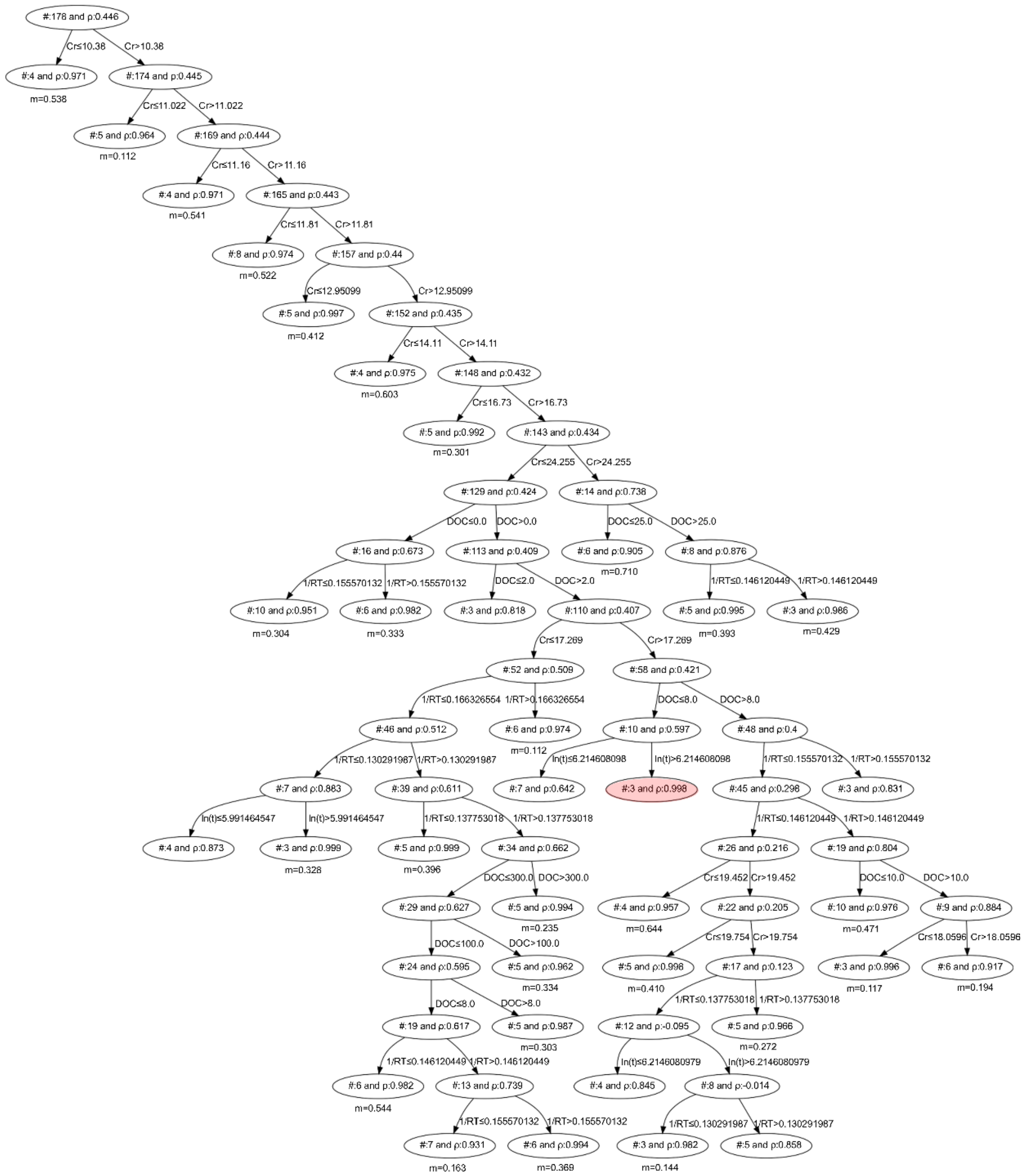

(b)

Figure S4. TCLR results (a) of $ln\frac{\Delta w}{\Delta w_{00}}$ versus 1/RT and (b) of $ln\frac{\Delta w}{\Delta w_{00}}$ versus ln(t/t0)

2.7 The sub-domains of leaves

Table S2. The sub-domains on each leaf of a certain time exponent

m	Cr/wt.%	T/K	DOC/bbp	time/h
0.538	10.38	773.15	8000	100-1000
0.112	11.022	923.15	0	200-1000
0.541	11.16	773.15	8000	100-1000
0.522	11.43-11.81	773.15	8000	100-1000
0.412	12.951	823.15	200	200-1000
0.603	14.11	773.15	8000	100-1000
0.301	16.73	773.15	0	200-1000
0.71	30.319	773.15	25	172-505
0.393	27.636	823.15	200	200-1000
0.429	30.319	773.15	2000	168-503
0.333	17.269	673.15	0	40-500
0.304	17.0882-19.48	773.15-823.15	0	110-1000
0.112	17.269	673.15	8	40-500
0.328	17.0882	923.15	8000	600-1000
0.396	17.0882	873.15	8000	200-1000
0.235	17.0882	823.15	2000	200-1000
0.334	17.0882	823.15	300	200-1000
0.303	17.0882	823.15	100	200-1000
0.544	17.269	823.15	8	50-500
0.163	17.269	773.15	8	50-500
0.369	17.269	723.15	8	30-500
0.471	18.06-22.321	773.15	10	350-2000
0.117	18.06	773.15	25	30-630
0.194	19.29-22.321	773.15	25	30-630
0.644	18.06-19.452	873.15-923.15	25-2000	320-1000
0.41	19.754	873.15	10	100-1500
0.272	24.255	823.15	10	100-1500

0.144	24.255	923.15	10	600-1500

Table S3. The sub-domains on each leaf of a certain activation energy

$Q/KJ \cdot mol^{-1}$	Cr/wt.%	T/K	DOC/bbp	time/h
79.42	17.269-22.321	673.15-773.15	8-25	30
76.35	11.022-19.48	673.15-923.15	0	40-1000
47.38	17.269-18.269	673.15-823.15	8	40-50
45.91	10.38-17.269	673.15-823.15	8-8000	100
43.38	10.38-17.0882	773.15-973.15	8000	200-1000
69.21	17.0882-30.319	773.15-923.15	2000	168-1000
139.18	27.636-30.319	773.15-823.15	25-200	172-200
112.4	27.636-30.319	773.15-823.15	25-200	333-1000
82.26	12.951-22.321	673.15-873.15	25-300	172-1000
57.39	17.269	673.15-823.15	8	150-500
66.59	18.2693-24.255	673.15-873.15	2-10	168-300
60.28	18.0596-22.321	673.15-773.15	2-10	335-500
65.96	18.2693-19.29	673.15-773.15	2-8	503-750
76.99	18.0596-19.754	773.15-873.15	10	600-2000
79.91	22.321-24.255	773.15-873.15	10	600-680
77.72	22.321-24.255	773.15-873.15	10	1000
124.72	19.754-24.255	823.15-873.15	10	100

2.8 The r value for the oxidation in deaerated SCW

Table S4. The r value for the oxidation in deaerated SCW (DOC<10ppb)

Time/h	DOC/ppb	α	r/ppb
40	0	528944.5	1.4
40	8	3639766	
100	0	543287	1.7
100	8	3121216	
200	0	594149.1	2.3
200	8	2648045	
300	0	591827	2.7
300	8	2373298	
400	0	508266.9	2.3
400	8	2276961	
500	0	562178.6	2.6
500	8	2290301	
Deaerated condition, Temperature=673.15K, $[\widetilde{Cr}]$=17.269wt.%, mean(r)=2.17			

The parameter $\alpha = \frac{\Delta w_0}{\Delta w_{00}}\left(\frac{(DOC+r)}{(DCO)_0}\right) = \alpha(T, t, [\widetilde{Cr}], DOC)$ is estimated on the entire region R_{Qm} by using the experimental data, where the DOC effect is expressed by $(DOC + r)/DOC_0$ and Δw_0 is independent with DOC. The slope of linear α vs. DOC yields value of Δw_0 and letting $DOC \to 0$ gives the r value. Table S4 shows the estimated r values with the mean $\frac{r}{(DCO)_0} = 2.17$.

3 Open-source address

The data, software and corresponding source code are fully open, available at following website: https://github.com/Bin-Cao/TCLRmodel.

Reference

[1] Zhang T-Y, Cao B, Zhang SY, Sun S, Tree-classifier for linear regression software [No.2021SR1951267] 2021.

[2] Reshef D N, Reshef Y A, Finucane H K, Grossman S R, McVean G, Turnbaugh P J, et al. Detecting novel associations in large data sets. *Science* 2011; 334: 1518-1524.

[3] Pedregosa F, Varoquaux G, Gramfort A, Michel V, Thirion B, Grisel O, et al. Scikit-learn: Machine learning in Python. *the Journal of machine Learning research* 2012; 12: 2825-2830.

[4] Gómez-Briceño D, Blázquez F, Sáez-Maderuelo A. Oxidation of austenitic and ferritic/martensitic alloys in supercritical water. *The Journal of Supercritical Fluids* 2013; 78: 103-113.

[5] Shen Z, Wang J M, Zhang L F. Corrosion Behaviors of Ferritic/Martenstic Steel and Austenitic Stainless Steel in Supercritical Water. *Journal of Shanghai Jiaotong University* 2015; 49: 1768-1777.

[6] Tan L, Ren X, Allen T R. Corrosion behavior of 9–12% Cr ferritic–martensitic steels in supercritical water. *Corrosion science* 2010; 52(4): 1520-1528.

[7] Zhong X, Wu X, Han E H. Effects of exposure temperature and time on corrosion behavior of a ferritic–martensitic steel P92 in aerated supercritical water. *Corrosion Science* 2015; 90: 511-521.

[8] Zhang N Q, Xu H, Li B R, Bai Y, Liu D Y. Influence of the dissolved oxygen content on corrosion of the ferritic–martensitic steel P92 in supercritical water. *Corrosion science* 2012; 56: 123-128.

[9] Chen Y, Sridharan K, Allen T. Corrosion behavior of ferritic–martensitic steel T91 in supercritical water. *Corrosion Science* 2006; 48(9): 2843-2854.

[10] Tan L, Anderson M, Taylor D, Allen T R. Corrosion of austenitic and ferritic-martensitic steels exposed to supercritical carbon dioxide. *Corrosion Science* 2011; 53(10): 3273-3280.

[11] Tan L, Machut M T, Sridharan K, Allen T R. Corrosion behavior of a ferritic/martensitic steel HCM12A exposed to harsh environments. *Journal of Nuclear Materials* 2007; 371(1-3): 161-170.

[12] Bischoff J, Motta A T, Eichfeld C, Comstock R J, Cao G, Allen T R. Corrosion of ferritic–martensitic steels in steam and supercritical water. *Journal of Nuclear Materials* 2013; 441(1-3): 604-611.

[13] Ren X, Sridharan K, Allen T R. Corrosion of ferritic–martensitic steel HT9 in supercritical water. *Journal of Nuclear Materials* 2006; 358(2-3): 227-234.

[14] Yin K, Qiu S, Tang R, Zhang Q, Zhang L. Corrosion behavior of ferritic/martensitic steel P92 in supercritical water. *The Journal of Supercritical Fluids* 2009; 50(3): 235-239.

[15] Li Y, Wang S, Sun P, Yang J, Tang X, Xu D, et al. Investigation on early formation and evolution of oxide scales on ferritic–martensitic steels in supercritical water. *Corrosion Science* 2018; 135: 136-146.

[16] Chen K, Zhang L, Shen Z. Understanding the surface oxide evolution of T91 ferritic-martensitic steel in supercritical water through advanced characterization. *Acta Materialia* 2020; 194: 156-167.

[17] Shi Q, Yan W, Li Y, Zhang N, Shan Y, Yang K, Abe H. Oxidation behavior of ferritic/martensitic steels in flowing supercritical water. *Journal of Materials Science & Technology* 2021; 64: 114-125.

[18] Gao WH, Shen Z, Zhang L. Corrosion Behavior of T91 Steel in Supercritical Water. *Corrosion &. Protection* 2016; 37(6): 444-502.

[19] Kaiju Y, Qiu S, Tang R, Zhang Q, Zhang L, Liu H. Characterization of the porosity of the oxide scales on ferritic-martensitic steel P91 and P92 exposed in supercritical water. *Journal of Chinese Society for Corrosion and protection* 2010; 30(1): 1-5.

[20] Qiao YX, Wang S, Gao YJ, Shi H, Tang R, Xu FJ. Corrosion behavior of ferritic-martensitic steel P92 in supercritical water. *Journal of Iron and Steel Research* 2016; 28(08): 57-63.

[21] Zhong X, Wu X, Hu H. Corrosion behaviors of nuclear-grade stainless steel and ferritic-martensitic steel in supercritical water. *Acta Metall Sinica* 2011; 47(7): 932-938.

[22] Shen Z, Duan ZG, Sun Y, Zhang LF, Xu XL. Corrosion Behavior of 12Cr-F/M Steel in Supercritical Water. *Corrosion &. Protection* 2014*;* 35(05): 434-437.

FMO-Dataset

Table S5. FM steel oxidation dataset

The detailed literatures are: Ref. [6], [4], [7], [8], [9], [10], [11], [12], [13], [14], [15], [16], [17], [18], [19], [20], [21], and [22].

(The document.csv can be download at https://github.com/Bin-Cao/TCLRmodel.)

Num.	Cr (wt.%)	Si (wt.%)	Mn (wt.%)	C (wt.%)	Ni (wt.%)	Mo (wt.%)	Nb (wt.%)	W (wt.%)	V (wt.%)	P (wt.%)	Cu (wt.%)	T (℃)	Pressure (MPa)	t(h)	DO (ppb)	Weightgain (mg/dm^2)
1	8.895	0.235	0.401	0.102	0.121	0.889	0.079	0	0.202	0.019	0.085	400	25	40	8	34
2	8.895	0.235	0.401	0.102	0.121	0.889	0.079	0	0.202	0.019	0.085	400	25	580	8	43
3	8.895	0.235	0.401	0.102	0.121	0.889	0.079	0	0.202	0.019	0.085	400	30	255	8	33
4	8.895	0.235	0.401	0.102	0.121	0.889	0.079	0	0.202	0.019	0.085	400	30	500	8	42
5	8.895	0.235	0.401	0.102	0.121	0.889	0.079	0	0.202	0.019	0.085	400	30	760	8	47
6	8.895	0.235	0.401	0.102	0.121	0.889	0.079	0	0.202	0.019	0.085	500	25	500	8	190
7	8.895	0.235	0.401	0.102	0.121	0.889	0.079	0	0.202	0.019	0.085	500	25	500	8	203
8	8.895	0.235	0.401	0.102	0.121	0.889	0.079	0	0.202	0.019	0.085	500	25	750	8	241
9	8.895	0.235	0.401	0.102	0.121	0.889	0.079	0	0.202	0.019	0.085	500	30	500	8	194
10	8.895	0.235	0.401	0.102	0.121	0.889	0.079	0	0.202	0.019	0.085	500	30	500	8	198
11	8.895	0.235	0.401	0.102	0.121	0.889	0.079	0	0.202	0.019	0.085	500	30	740	8	196

12	8.96	0.18	0.5	0.12	0.13	0.36	0.068	1.75	0.18	0.013	0	400	25	40	8	50
13	8.96	0.18	0.5	0.12	0.13	0.36	0.068	1.75	0.18	0.013	0	400	25	100	8	57.01
14	8.96	0.18	0.5	0.12	0.13	0.36	0.068	1.75	0.18	0.013	0	400	25	200	8	60
15	8.96	0.18	0.5	0.12	0.13	0.36	0.068	1.75	0.18	0.013	0	400	25	300	8	61
16	8.96	0.18	0.5	0.12	0.13	0.36	0.068	1.75	0.18	0.013	0	400	25	400	8	64
17	8.96	0.18	0.5	0.12	0.13	0.36	0.068	1.75	0.18	0.013	0	400	25	500	8	69
18	8.96	0.18	0.5	0.12	0.13	0.36	0.068	1.75	0.18	0.013	0	450	25	30	8	70
19	8.96	0.18	0.5	0.12	0.13	0.36	0.068	1.75	0.18	0.013	0	450	25	100	8	120.1
20	8.96	0.18	0.5	0.12	0.13	0.36	0.068	1.75	0.18	0.013	0	450	25	200	8	145
21	8.96	0.18	0.5	0.12	0.13	0.36	0.068	1.75	0.18	0.013	0	450	25	300	8	161
22	8.96	0.18	0.5	0.12	0.13	0.36	0.068	1.75	0.18	0.013	0	450	25	400	8	182.02
23	8.96	0.18	0.5	0.12	0.13	0.36	0.068	1.75	0.18	0.013	0	450	25	500	8	210.1
24	8.96	0.18	0.5	0.12	0.13	0.36	0.068	1.75	0.18	0.013	0	500	25	50	8	180
25	8.96	0.18	0.5	0.12	0.13	0.36	0.068	1.75	0.18	0.013	0	500	25	100	8	175
26	8.96	0.18	0.5	0.12	0.13	0.36	0.068	1.75	0.18	0.013	0	500	25	150	8	200
27	8.96	0.18	0.5	0.12	0.13	0.36	0.068	1.75	0.18	0.013	0	500	25	200	8	210.2
28	8.96	0.18	0.5	0.12	0.13	0.36	0.068	1.75	0.18	0.013	0	500	25	270	8	230
29	8.96	0.18	0.5	0.12	0.13	0.36	0.068	1.75	0.18	0.013	0	500	25	380	8	250

30	8.96	0.18	0.5	0.12	0.13	0.36	0.068	1.75	0.18	0.013	0	500	25	500	8	240.1
31	8.96	0.18	0.5	0.12	0.13	0.36	0.068	1.75	0.18	0.013	0	550	25	50	8	160
32	8.96	0.18	0.5	0.12	0.13	0.36	0.068	1.75	0.18	0.013	0	550	25	100	8	283
33	8.96	0.18	0.5	0.12	0.13	0.36	0.068	1.75	0.18	0.013	0	550	25	200	8	421
34	8.96	0.18	0.5	0.12	0.13	0.36	0.068	1.75	0.18	0.013	0	550	25	310	8	501
35	8.96	0.18	0.5	0.12	0.13	0.36	0.068	1.75	0.18	0.013	0	550	25	400	8	539
36	8.96	0.18	0.5	0.12	0.13	0.36	0.068	1.75	0.18	0.013	0	550	25	500	8	565
37	8.63	0.38	0.42	0.1	0.15	0.37	0.053	1.59	0.164	0.014	0.09	550	25	110	0	120.2
38	8.63	0.38	0.42	0.1	0.15	0.37	0.053	1.59	0.164	0.014	0.09	550	25	460	0	192
39	8.63	0.38	0.42	0.1	0.15	0.37	0.053	1.59	0.164	0.014	0.09	550	25	600	0	205.01
40	8.63	0.38	0.42	0.1	0.15	0.37	0.053	1.59	0.164	0.014	0.09	550	25	780	0	228
41	8.63	0.38	0.42	0.1	0.15	0.37	0.053	1.59	0.164	0.014	0.09	550	25	1000	0	241.001
42	8.63	0.38	0.42	0.1	0.15	0.37	0.053	1.59	0.164	0.014	0.09	550	25	200	100	181.01
43	8.63	0.38	0.42	0.1	0.15	0.37	0.053	1.59	0.164	0.014	0.09	550	25	400	100	227
44	8.63	0.38	0.42	0.1	0.15	0.37	0.053	1.59	0.164	0.014	0.09	550	25	600	100	270.2
45	8.63	0.38	0.42	0.1	0.15	0.37	0.053	1.59	0.164	0.014	0.09	550	25	800	100	272.01
46	8.63	0.38	0.42	0.1	0.15	0.37	0.053	1.59	0.164	0.014	0.09	550	25	1000	100	295.1
47	8.63	0.38	0.42	0.1	0.15	0.37	0.053	1.59	0.164	0.014	0.09	550	25	200	300	205.02

48	8.63	0.38	0.42	0.1	0.15	0.37	0.053	1.59	0.164	0.014	0.09	550	25	400	300	240.2
49	8.63	0.38	0.42	0.1	0.15	0.37	0.053	1.59	0.164	0.014	0.09	550	25	600	300	317.5
50	8.63	0.38	0.42	0.1	0.15	0.37	0.053	1.59	0.164	0.014	0.09	550	25	800	300	334
51	8.63	0.38	0.42	0.1	0.15	0.37	0.053	1.59	0.164	0.014	0.09	550	25	1000	300	330.2
52	8.63	0.38	0.42	0.1	0.15	0.37	0.053	1.59	0.164	0.014	0.09	550	25	200	2000	271
53	8.63	0.38	0.42	0.1	0.15	0.37	0.053	1.59	0.164	0.014	0.09	550	25	400	2000	319
54	8.63	0.38	0.42	0.1	0.15	0.37	0.053	1.59	0.164	0.014	0.09	550	25	600	2000	352.5
55	8.63	0.38	0.42	0.1	0.15	0.37	0.053	1.59	0.164	0.014	0.09	550	25	800	2000	365
56	8.63	0.38	0.42	0.1	0.15	0.37	0.053	1.59	0.164	0.014	0.09	550	25	1000	2000	402
57	9.5	0.5	0.5	0.13	0.4	0.6	0.06	2	0.25	0.02	0.25	550	31	100	10	118.4
58	9.5	0.5	0.5	0.13	0.4	0.6	0.06	2	0.25	0.02	0.25	550	31	300	10	195.1
59	9.5	0.5	0.5	0.13	0.4	0.6	0.06	2	0.25	0.02	0.25	550	31	600	10	211
60	9.5	0.5	0.5	0.13	0.4	0.6	0.06	2	0.25	0.02	0.25	550	31	1000	10	234.7
61	9.5	0.5	0.5	0.13	0.4	0.6	0.06	2	0.25	0.02	0.25	550	31	1500	10	254.8
62	9.5	0.5	0.5	0.13	0.4	0.6	0.06	2	0.25	0.02	0.25	600	31	100	10	351
63	9.5	0.5	0.5	0.13	0.4	0.6	0.06	2	0.25	0.02	0.25	600	31	300	10	500.1
64	9.5	0.5	0.5	0.13	0.4	0.6	0.06	2	0.25	0.02	0.25	600	31	600	10	638.1
65	9.5	0.5	0.5	0.13	0.4	0.6	0.06	2	0.25	0.02	0.25	600	31	1000	10	745.7

66	9.5	0.5	0.5	0.13	0.4	0.6	0.06	2	0.25	0.02	0.25	600	31	1500	10	781.1
67	9.5	0.5	0.5	0.13	0.4	0.6	0.06	2	0.25	0.02	0.25	650	31	300	10	111.561
68	9.5	0.5	0.5	0.13	0.4	0.6	0.06	2	0.25	0.02	0.25	650	31	600	10	129.41
69	9.5	0.5	0.5	0.13	0.4	0.6	0.06	2	0.25	0.02	0.25	650	31	1000	10	136.36
70	9.5	0.5	0.5	0.13	0.4	0.6	0.06	2	0.25	0.02	0.25	650	31	1500	10	147.9
71	8.37	0.28	0.45	0.1	0.21	0.9	0.076	0	0.216	0.009	0.17	500	25	505	25	187
72	8.37	0.28	0.45	0.1	0.21	0.9	0.076	0	0.216	0.009	0.17	500	25	333	25	173
73	8.37	0.28	0.45	0.1	0.21	0.9	0.076	0	0.216	0.009	0.17	500	25	172	25	120.3
74	8.37	0.28	0.45	0.1	0.21	0.9	0.076	0	0.216	0.009	0.17	500	25	503	2	163
75	8.37	0.28	0.45	0.1	0.21	0.9	0.076	0	0.216	0.009	0.17	500	25	335	2	181.02
76	8.37	0.28	0.45	0.1	0.21	0.9	0.076	0	0.216	0.009	0.17	500	25	168	2	118
77	8.37	0.28	0.45	0.1	0.21	0.9	0.076	0	0.22	0.009	0.17	650	20.7	500	2000	818
78	10.83	0.27	0.64	0.11	0.39	0.3	0.054	1.89	0.19	0.016	1.02	500	25	350	10	121.01
79	10.83	0.27	0.64	0.11	0.39	0.3	0.054	1.89	0.19	0.016	1.02	500	25	680	10	151
80	10.83	0.27	0.64	0.11	0.39	0.3	0.054	1.89	0.19	0.016	1.02	500	25	1000	10	183
81	10.83	0.27	0.64	0.11	0.39	0.3	0.054	1.89	0.19	0.016	1.02	500	25	1300	10	191
82	10.83	0.27	0.64	0.11	0.39	0.3	0.054	1.89	0.19	0.016	1.02	500	25	2000	10	272.02
83	8.82	0.102	0.45	0.109	0.174	0.468	0.064	1.87	0.194	0.012	0	500	25	350	10	122.01

84	8.82	0.102	0.45	0.109	0.174	0.468	0.064	1.87	0.194	0.012	0	500	25	680	10	151
85	8.82	0.102	0.45	0.109	0.174	0.468	0.064	1.87	0.194	0.012	0	500	25	1000	10	202.01
86	8.82	0.102	0.45	0.109	0.174	0.468	0.064	1.87	0.194	0.012	0	500	25	1300	10	232
87	8.82	0.102	0.45	0.109	0.174	0.468	0.064	1.87	0.194	0.012	0	500	25	2000	10	281
88	10.83	0.27	0.64	0.11	0.39	0.3	0.054	1.89	0.19	0.016	1.02	360	25	320	25	20.892961
89	10.83	0.27	0.64	0.11	0.39	0.3	0.054	1.89	0.19	0.016	1.02	360	25	630	25	5.1286138
90	10.83	0.27	0.64	0.11	0.39	0.3	0.054	1.89	0.19	0.016	1.02	400	25	30	25	17.782794
91	10.83	0.27	0.64	0.11	0.39	0.3	0.054	1.89	0.19	0.016	1.02	400	25	320	25	20.417379
92	10.83	0.27	0.64	0.11	0.39	0.3	0.054	1.89	0.19	0.016	1.02	400	25	400	25	25.703958
93	10.83	0.27	0.64	0.11	0.39	0.3	0.054	1.89	0.19	0.016	1.02	500	25	30	25	107.15193
94	10.83	0.27	0.64	0.11	0.39	0.3	0.054	1.89	0.19	0.016	1.02	500	25	320	25	169.82437
95	10.83	0.27	0.64	0.11	0.39	0.3	0.054	1.89	0.19	0.016	1.02	500	25	630	25	177.82794
96	10.83	0.27	0.64	0.11	0.39	0.3	0.054	1.89	0.19	0.016	1.02	600	25	320	25	549.54087
97	10.83	0.27	0.64	0.11	0.39	0.3	0.054	1.89	0.19	0.016	1.02	600	25	630	25	602.55959
98	10.83	0.27	0.64	0.11	0.39	0.3	0.054	1.89	0.19	0.016	1.02	600	25	1000	25	646.01
99	8.82	0.102	0.45	0.109	0.174	0.468	0.064	1.87	0.194	0	0	360	25	320	25	10.471285
100	8.82	0.102	0.45	0.109	0.174	0.468	0.064	1.87	0.194	0	0	500	25	30	25	128.82496
101	8.82	0.102	0.45	0.109	0.174	0.468	0.064	1.87	0.194	0	0	500	25	320	25	173.78008

102	8.82	0.102	0.45	0.109	0.174	0.468	0.064	1.87	0.194	0	0	500	25	630	25	182.01
103	8.82	0.102	0.45	0.109	0.174	0.468	0.064	1.87	0.194	0	0	600	25	320	25	646.02
104	8.82	0.102	0.45	0.109	0.174	0.468	0.064	1.87	0.194	0	0	600	25	630	25	831.76377
105	11.94	0.3	0.69	0.21	0.62	1.03	0	0.48	0.3	0.013	0.02	500	25	168	2000	141
106	11.94	0.3	0.69	0.21	0.62	1.03	0	0.48	0.3	0.013	0.02	500	25	335	2000	202.02
107	11.94	0.3	0.69	0.21	0.62	1.03	0	0.48	0.3	0.013	0.02	500	25	503	2000	223
108	11.94	0.3	0.69	0.21	0.62	1.03	0	0.48	0.3	0.013	0.02	500	25	172	25	72
109	11.94	0.3	0.69	0.21	0.62	1.03	0	0.48	0.3	0.013	0.02	500	25	333	25	121.02
110	11.94	0.3	0.69	0.21	0.62	1.03	0	0.48	0.3	0.013	0.02	500	25	505	25	122.02
111	11.94	0.3	0.69	0.21	0.62	1.03	0	0.48	0.3	0.013	0.02	500	25	172	25	57
112	11.94	0.3	0.69	0.21	0.62	1.03	0	0.48	0.3	0.013	0.02	500	25	333	25	137
113	11.94	0.3	0.69	0.21	0.62	1.03	0	0.48	0.3	0.013	0.02	500	25	505	25	144
114	11.75	0.15	0.45	0.095	0	0	0	2.75	0.2	0	0	500	24.8	200	0	129
115	11.75	0.15	0.45	0.095	0	0	0	2.75	0.2	0	0	500	24.8	400	0	162
116	11.75	0.15	0.45	0.095	0	0	0	2.75	0.2	0	0	500	24.8	600	0	181
117	11.75	0.15	0.45	0.095	0	0	0	2.75	0.2	0	0	500	24.8	800	0	198
118	11.75	0.15	0.45	0.095	0	0	0	2.75	0.2	0	0	500	24.8	1000	0	207
119	9	0.15	0.45	0.115	0	0	0	2	0.2	0	0	500	24.8	200	0	131

120	9	0.15	0.45	0.115	0	0	0	2	0.2	0	0	500	24.8	400	0	171
121	9	0.15	0.45	0.115	0	0	0	2	0.2	0	0	500	24.8	600	0	189
122	9	0.15	0.45	0.115	0	0	0	2	0.2	0	0	500	24.8	800	0	202
123	9	0.15	0.45	0.115	0	0	0	2	0.2	0	0	500	24.8	1000	0	214
124	11.25	0.225	0.9	0.135	0	0	0	2.4	0.015	0.005	0	650	25	200	0	510
125	11.25	0.225	0.9	0.135	0	0	0	2.4	0.015	0.005	0	650	25	400	0	565
126	11.25	0.225	0.9	0.135	0	0	0	2.4	0.015	0.005	0	650	25	600	0	601
127	11.25	0.225	0.9	0.135	0	0	0	2.4	0.015	0.005	0	650	25	800	0	591
128	11.25	0.225	0.9	0.135	0	0	0	2.4	0.015	0.005	0	650	25	1000	0	615
129	8.96	0.18	0.5	0.12	0.13	0.36	0.068	1.75	0.18	0.013	0	400	25	40	0	8
130	8.96	0.18	0.5	0.12	0.13	0.36	0.068	1.75	0.18	0.013	0	400	25	100	0	11
131	8.96	0.18	0.5	0.12	0.13	0.36	0.068	1.75	0.18	0.013	0	400	25	200	0	15
132	8.96	0.18	0.5	0.12	0.13	0.36	0.068	1.75	0.18	0.013	0	400	25	300	0	17
133	8.96	0.18	0.5	0.12	0.13	0.36	0.068	1.75	0.18	0.013	0	400	25	400	0	16
134	8.96	0.18	0.5	0.12	0.13	0.36	0.068	1.75	0.18	0.013	0	400	25	500	0	19
135	11.1	0.7	0.6	0	0	0	0	0	0	0	0	500	25	100	8000	177.2
136	11.1	0.7	0.6	0	0	0	0	0	0	0	0	500	25	250	8000	333.3
137	11.1	0.7	0.6	0	0	0	0	0	0	0	0	500	25	500	8000	436.9

138	11.1	0.7	0.6	0	0	0	0	0	0	0	0	500	25	1000	8000	546.3
139	11.2	0.7	1.1	0	0	0	0	0	0	0	0	500	25	100	8000	182.4
140	11.2	0.7	1.1	0	0	0	0	0	0	0	0	500	25	250	8000	372.9
141	11.2	0.7	1.1	0	0	0	0	0	0	0	0	500	25	500	8000	539.9
142	11.2	0.7	1.1	0	0	0	0	0	0	0	0	500	25	1000	8000	620.3
143	11.6	1.1	1.8	0	0	0	0	0	0	0	0	500	25	100	8000	158.7
144	11.6	1.1	1.8	0	0	0	0	0	0	0	0	500	25	250	8000	341.3
145	11.6	1.1	1.8	0	0	0	0	0	0	0	0	500	25	500	8000	473.9
146	11.6	1.1	1.8	0	0	0	0	0	0	0	0	500	25	1000	8000	570.1
147	11.6	2.2	1.7	0	0	0	0	0	0	0	0	500	25	100	8000	129.6
148	11.6	2.2	1.7	0	0	0	0	0	0	0	0	500	25	250	8000	296.4
149	11.6	2.2	1.7	0	0	0	0	0	0	0	0	500	25	500	8000	410.5
150	11.6	2.2	1.7	0	0	0	0	0	0	0	0	500	25	1000	8000	522.5
151	11.7	0.6	1.8	0	0	0	0	0	0	0	0	500	25	100	8000	179.8
152	11.7	0.6	1.8	0	0	0	0	0	0	0	0	500	25	250	8000	391.4
153	11.7	0.6	1.8	0	0	0	0	0	0	0	0	500	25	500	8000	489.7
154	11.7	0.6	1.8	0	0	0	0	0	0	0	0	500	25	1000	8000	636.1
155	8.63	0.38	0.42	0.1	0.15	0.0013	0.053	1.59	0.164	0.014	0	600	25	200	8000	622.3

156	8.63	0.38	0.42	0.1	0.15	0.0013	0.053	1.59	0.164	0.014	0	600	25	400	8000	838
157	8.63	0.38	0.42	0.1	0.15	0.0013	0.053	1.59	0.164	0.014	0	600	25	600	8000	983
158	8.63	0.38	0.42	0.1	0.15	0.0013	0.053	1.59	0.164	0.014	0	600	25	800	8000	1074.9
159	8.63	0.38	0.42	0.1	0.15	0.0013	0.053	1.59	0.164	0.014	0	600	25	1000	8000	1184.5
160	8.63	0.38	0.42	0.1	0.15	0.0013	0.053	1.59	0.164	0.014	0	650	25	200	8000	1205.8
161	8.63	0.38	0.42	0.1	0.15	0.0013	0.053	1.59	0.164	0.014	0	650	25	400	8000	1474.5
162	8.63	0.38	0.42	0.1	0.15	0.0013	0.053	1.59	0.164	0.014	0	650	25	600	8000	1584
163	8.63	0.38	0.42	0.1	0.15	0.0013	0.053	1.59	0.164	0.014	0	650	25	800	8000	1729.1
164	8.63	0.38	0.42	0.1	0.15	0.0013	0.053	1.59	0.164	0.014	0	650	25	1000	8000	1874.1
165	8.63	0.38	0.42	0.1	0.15	0.0013	0.053	1.59	0.164	0.014	0	700	25	200	8000	1294.1
166	8.63	0.38	0.42	0.1	0.15	0.0013	0.053	1.59	0.164	0.014	0	700	25	400	8000	1792.7
167	9.03	0.22	0.41	0.099	0	0	0	2.02	0.1	0.005	0	550	25	200	200	302.293
168	9.03	0.22	0.41	0.099	0	0	0	2.02	0.1	0.005	0	550	25	400	200	398.866
169	9.03	0.22	0.41	0.099	0	0	0	2.02	0.1	0.005	0	550	25	600	200	461.764
170	9.03	0.22	0.41	0.099	0	0	0	2.02	0.1	0.005	0	550	25	800	200	520.904
171	9.03	0.22	0.41	0.099	0	0	0	2.02	0.1	0.005	0	550	25	1000	200	598.76
172	12	0.17	1	0.1	1	1	0	1.1	0.15	0.005	0	550	25	200	200	238.658
173	12	0.17	1	0.1	1	1	0	1.1	0.15	0.005	0	550	25	400	200	312.787

174	12	0.17	1	0.1	1	1	0	1.1	0.15	0.005	0	550	25	600	200	353.195
175	12	0.17	1	0.1	1	1	0	1.1	0.15	0.005	0	550	25	800	200	401.121
176	12	0.17	1	0.1	1	1	0	1.1	0.15	0.005	0	550	25	1000	200	460.261
177	8.93	0.25	0.45	0.092	0.23	0.82	0	0	0.21	0.012	0.18	600	25	100	10	322
178	8.93	0.25	0.45	0.092	0.23	0.82	0	0	0.21	0.012	0.18	600	25	300	10	539
179	8.93	0.25	0.45	0.092	0.23	0.82	0	0	0.21	0.012	0.18	600	25	600	10	695
180	8.93	0.25	0.45	0.092	0.23	0.82	0	0	0.21	0.012	0.18	600	25	1000	10	836
181	8.93	0.25	0.45	0.092	0.23	0.82	0	0	0.21	0.012	0.18	600	25	1500	10	993
182	8.82	0.102	0.45	0.109	0.174	0.468	0.064	1.87	0.194	0	0	600	25	1000	25	1380.3843
183	10.83	0.27	0.64	0.11	0.39	0.3	0.054	1.89	0.19	0.009	1.02	650	20.7	500	2000	1380.01
184	9.5	0.5	0.5	0.13	0.4	0.6	0.06	2	0.25	0.02	0.25	650	31	100	10	869.7